3.1 MODELING URBAN HEAT ISLANDS IN CALIFORNIA CENTRAL VALLEY

L. Bereket[1], J.E. González[1,*], D. Fabris[1], N.L. Miller[2], and C. Milesi[3]
[1]Clara University, Santa Clara, CA 95053,
[2]Lawrence Berkeley National Laboratory, [3]NASA Ames Research Center

(08 November 2005)

1. INTRODUCTION

Urban heat islands (UHI) have been extensively studied using observational data (*e.g.* Bornstein 1968; Price 1979; Landsberg, 1981; Gallo *et al.*, 1993; Tso, 1995; Jauregui, 1997; Lo *et al.* 1997) and numerical simulations (*e.g.* Myrup 1969; Dixon *et al.* 2003). Urban growth, anthropogenic heat generation, and global warming contribute to increasing urban temperatures and associated health dangers: heat stroke for the elderly and pollution for the general population. The development of urban heat islands (Bornstein, 1995) will have lasting effect on energy usage through air-conditioning, water usage and resource allocation, and general urban planning. heating effects are mitigated by local climate and weather patterns, and implementation of energy efficiency and renewable energy measures. The current collaborative work between Santa Clara University, Lawrence Berkeley National Laboratory, San Jose State University and NASA Ames, has identified local heating trends for San Jose and northern San Joaquin Valley cities. The long-term climatology maps showed an increase of temperature trends by an average 1-3 ^{o}F over the locations considered at an average rate of 0.5^{o}F per decade in the northern San Joaquin valley cities (Lebassi *et al.* 2005). Modesto and Sacramento had shown a similar pattern of increase in temperature while San Jose had the highest rate of increase. This problem is of particular importance since urban growth has accelerated rapidly in the California Central and San Joaquin Valleys exposing larger populations to high levels of heat and air pollution. To improve the predicting capabilities for these processes, to ameliorate human effects, and to outline better urban growth, it is necessary to develop detailed micro scale atmospheric models of urban settings dynamically coupled to regional models.

This research paper focuses on the impact of the heat island on the Northern San Joaquin Valley (SJV) cities in general and Sacramento city in particular.

* *Corresponding author address:* Jorge Gonzalez Cruz, Santa Clara University, Dept. of Mechanical Engineering, Santa Clara, CA, 95053; e-mail jgonzalezcruz@scu.edu

The project will evaluate the impact of further urban growth relative to the local weather circulation patterns. To provide an understanding of the dynamics in the region, the mesoscale atmospheric modeling system (RAMS) will be used. The research is designated to extend understanding of the processes underlying the fundamental energetics and the partitioning of the energy at the urban-atmosphere interface. The effect of the sea breeze on the heat island will also be considered as the city of Sacramento is located open to the flow through the Carquinez strait.

2. SEA BREEZE OVERVIEW

The sea breeze is a mesoscale phenomenon that has been intensively studied. The sea breeze plays a key role in controlling meteorological conditions along coastal areas. Previous investigators have discussed the importance of the sea breeze for problems such as air pollution and smog transport, location and initiation of convection, aviation safety, gliding, sailing and surfing, and forest fire forecasting (Simpson 1994). The sea breeze is driven by the temperature differences between the land and ocean, and consists of onshore flow during the day (sea breeze) and offshore flow during the night (land breeze).

There are a diversity of factors that can affect the existence, strength, form, and evolution of sea breeze flows. Coastline shape can either enhance or inhibit sea breeze development. For example, the merging of two sea breezes originating from both sides of a peninsula enhances convection (Pielke 1974). On the other hand, over land areas adjoining bays, the sea breeze tends to diverge, which enhances low-level sinking motion, thus reducing cloud cover.

3. RAMS OVERVIEW

The mesoscale model used in this work is the Regional Atmospheric Modeling System (RAMS). RAMS is a highly versatile non-hydrostatic numerical model developed at Colorado State University. It solves the Reynolds-averaged primitive equations, which are described by Tripoli and Cotton (1986). The model uses a quasi-Boussinesq approximation, and "time-split" time differencing (Pielke 1984) and the Arakawa C staggered grid in which thermodynamic and moisture variables are defined at the grid volume center, and velocity components are defined at half grid points (Mesinger and Arakawa 1976). A Polar stereographic map projection is used for the horizontal grid domain, and a terrain-following sigma coordinate system with variable grid spacing is used in the vertical in order to increase the resolution near the surface The RAMS model can be initialized as variable field model initialization, where the four dimensional data assimilation (4DDA) uses time series of gridded variables of horizontal wind, potential temperature, and relative humidity values that are analyzed from either observations or large-scale model forecasts (e.g. NCEP, ETA).

3. SYNOPTIC CONDITIONS

The North Central California coastal region during spring and summer is characterized by northwesterly flow, which arises due to the high pressure system sitting over the northeastern Pacific about 1000 km northwest of the California coast, and a thermal low pressure centered over the southwestern United States desert. Subsidence associated with the Pacific high, coupled with the turbulent mixed marine layer, results in a strong inversion on the top of the MPBL (Burk and Thompson, 1996). The dynamics of this region is further complicated by the existence of a low level jet (LLJ) centered at 300-700m above the sea surface along the coast. The core of the jet lies within the strong steeply sloped inversion at the top of the MPBL (Bridger et al. 1993).

During our simulation period (16-19 June 2005) the synoptic conditions did not present significant variations over the San Francisco Bay Area except for the first day in which there was a light rain. The next three days of the simulation period were characterized by an offshore flow and relatively stable atmospheric conditions.

4. METHODOLOGY

4.1 Methodology Overview

Simulations with RAMS (version 4.4) have been performed for the research study in this paper. For all cases, a four day simulation period was chosen based on the Naval Postgraduate School (NPS) wind profiler data from Fort Ord. All simulations cover the period 0000 UTC 16-19 June 2005. These two cases were chosen so that the simulations would be comparable to the most detailed available observational climatological study of the northern San Joaquin Valley by Lebassi *et al.* (2005). In the climatology study, the highlighted heat island cases were those of summer months of June, July and August. RAMS simulations of the two cases were conducted, and model results were validated against and compare to observational data. The results were then examined for the existence of heat Island in Sacramento.

4.2 Case Description

The two case studies in this work are designed to examine relevant unsolved problems. Previous observational research has been able to detect a heating trend of the Northern Central Valley cities (Lebassi *et. al.* 2005) in the case of summertime months of June, July and August. We now used the Regional Atmospheric Simulation System (RAMS) to answer the outstanding questions about the urban heat island in Northern Central Valley and the effect of the heat island on the sea breeze from Central California. This region has bays with a non-linear coast and complex inland topography that can influence both the sea breeze and the urban heat island. Our center of model is the city of Sacramento. A four day simulation period was chosen in the month of June 2005 to simulate two cases represented by two different land use scenarios. The first land use scenario represents the current structure of the city of Sacramento hereafter called *Case 1*.

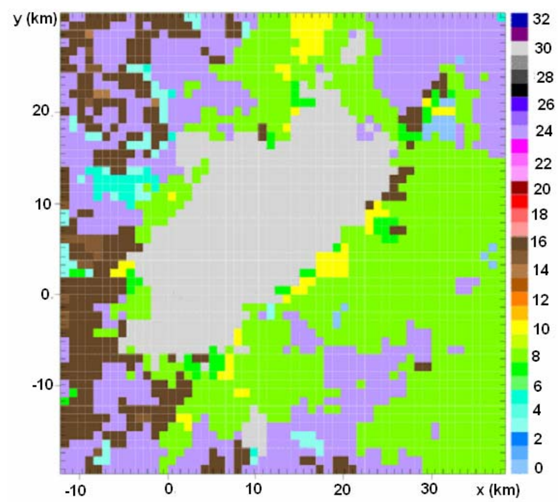

Fig. 1 Land use map for case 1 (30 is urban, which is represented by the gray area, 6 is short grass)

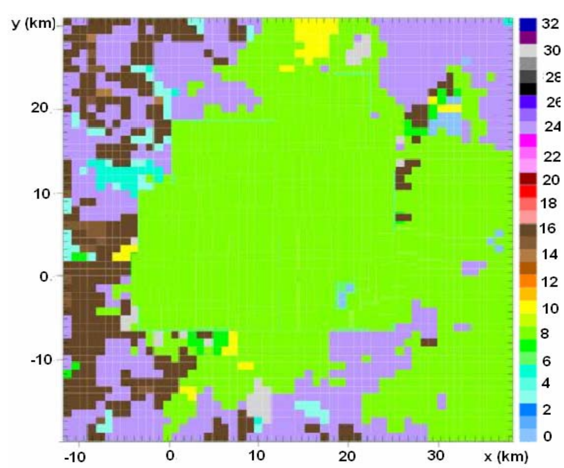

Fig. 2 Land use map for case 2 (30 is urban, which is represented by the gray area, 6, green is short grass)

The second case simulation modified the urban land use structure of the city of Sacrament to reflect the pre-urbanization 60 years ago, hereafter will refer to this case as *Case 2* (Fig. 2). The only change made in case 2 from case one was modification of the urban to short grass land use in the location of the city of Sacramento. As a result all the thermal properties of the urban were modified to correspond to those of short grass.

4.3 Model Setup

The RAMS simulations focused on the analysis of the heat island in northern California Central Valley. For this purpose, a nested-grid configuration was implemented. The outer model domain was extended eastward to include most of the western United States, and westward a considerable distance seaward (Fig. 3). Finer nested grids were applied over the area of interest in order to obtain meteorological fields at high resolution.

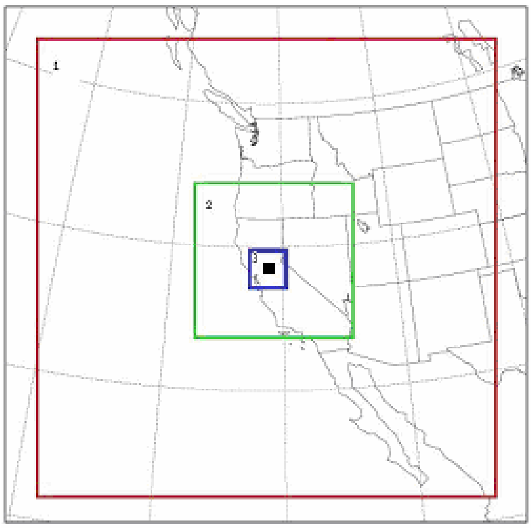

Fig. 3 Nested grid configuration of the modeled region. (grid 1: red, grid 2: green, gird 3: blue, grid 4: black)

Four nested grids were chosen to select important physical features of the meteorology. The domain for the outer grid was set to be large enough to capture the synoptic high pressure systems important for our three simulation cases. The second grid was selected to capture the Sierra Nevada mountain range and its influence on the dynamics, and the third grid was chosen to resolve the details of the coastal mountains near Sacramento. The fourth grid focused on the city of Sacramento itself. The detailed configuration that was selected and applied to the specified periods of simulation is summarized on table 1. All grids were centred at the domain coordinate of 36.80^o N and 120.78^o W (Sacramento). Concerning the vertical structure, the grids were identical. In detail, 50 vertical layers with grids above the first level increase by a grid stretch ratio of 1.2 and 10m initial resolution had been used.

Grid	NX	NY	NZ	$\Delta x, \Delta y$	Δz	Δt
1	80	80	30	60 km	30 m	10 s
2	82	82	30	15 km	30 m	5 s
3	70	70	30	2.5 km	30 m	2.5 s
4	54	54	30	0.9 km	30 m	2.5 s

Table 1: Model Grid Configuration

The vertical resolution was dense in the lower levels, and became increasingly coarse toward the top of the domain, which was set at 30 km.

4.4 Initialization and Input Data

Initialization of the RAMS simulations requires four types of input data: (1) topographic data that characterizes the elevation of the land surfaces; (2) sea surface temperature data that provides the temperature of the sea surface over the Pacific Ocean; (3) vegetation data that characterizes land surface characteristics; and (4) meteorological data that characterizes meteorological fields at the initial time, at the boundaries, and at synoptic distance scales. We describe each of these inputs in turn.

Topography files: The USGS topography data set of 30 arc-seconds (about 1 km) resolution was used.

SST files: The sea surface temperature (SST) data set from RAMS consists of mean climatologically monthly values with a resolution of 1 degree (about 100 km).

Vegetation files: The vegetation data set was in gridded form with a resolution of 30 arc-seconds (about 1 km) and global coverage. The vegetation data have been retrieved from the USGS. The USGS dataset is based on 1-km Advanced Very High Resolution Radiometer (AVHRR) data spanning April 1992 through March 1993 (www.atmet.com).

Meteorological fields: The model was initialized with gridded data sets prepared by the isentropic analysis package embedded in RAMS. The primary meteorological data was retrieved from the National Center for Environmental Prediction (NCEP). Their horizontal increment is 0.5 degree, and data are available every 6 hours (0000, 0600, 1200 and 1800 UTC). In addition, sounding and surface meteorological data from the University of Wyoming were used for model initialization and validation. The lateral boundary conditions on the outer grid followed the Klemp-Lilly condition, which is a variant of the Orlanski condition (Klemp *et. al.* 1978). Here, gravity wave propagation speeds computed for each model cell are averaged vertically, with the single average value being applied over the entire vertical column. The horizontal diffusion coefficients were computed as the product of the horizontal deformation rate and a length scale squared, based on the original Smagorinsky (1963) formulation. The vertical diffusion coefficients were computed according to the Mellor and Yamada (1974) parameterization scheme, which employs a prognostic turbulent kinetic energy variable. For both shortwave and long wave radiation parameterizations, the scheme described by Mahrer and Pielke (1977) has been used.

The roughness length is defined according to the vegetation cover. The simulation also allowed for the condensation of water vapor to cloud water, and the microphysical parameterization of any species of liquid or ice. The mean rain, snow, aggregate, graupel or hail droplet diameter was specified from the default value in the RAMS code. The number concentration is diagnosed automatically from this mean diameter and the forecast mixing ratio.

5. RESULTS

5.1 Model Validation

In order to lend confidence in the simulations, a validation of the model results against available observations was carried out. For the specified simulation period, the model reproduced the synoptic scale forcing, namely the locations of the high and low pressure systems with good accuracy. To gain insights into how well the model simulation depicted the thermal forcing of the low-level flow, the model surface temperature and wind speed fields were also compared to observations. Time series of surface temperature (hereafter temperature) of the station at Sacramento city was examined. The station at Sacramento was taken as a representative station the inland valley.

The model captured the day and night temperatures very well with the exception of the morning daytime spikes observed on the second and third days. At the Sacramento station (Fig. 4), both the daytime and nighttime model temperatures were in good agreement with observations except for small deviations just before sunrise on the third and fourth nights of the simulation. This could be attributed to the proximity of the stations to the Carquinez Strait, which allows cool, foggy air from the Pacific to create a strong nighttime inversion near the ground in the Central Valley near the California Bay-Delta. The first day peak in temperature was washed out due to light rain on that day. At the inland valley stations of Sacramento, time series plot of the comparison of model versus observation of daytime/night wind speed showed good agreement as well (Fig. 5). The Oakland sounding station was used also to validate the vertical profile of the simulation setup. Comparison plots of model and observationw at the Oakland airport were also in good agreement (not shown). The model had captured the inversions and stabilities in the vertical profile.

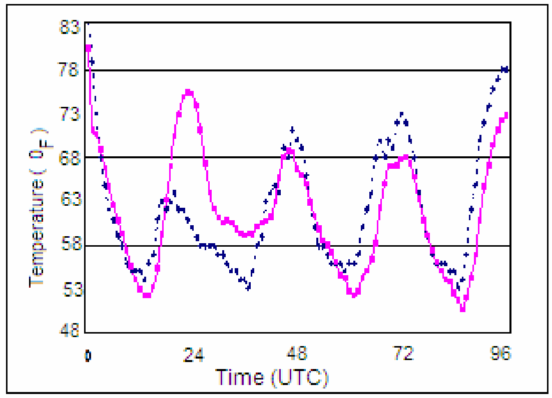

Fig. 4 Model versus observation 2 m temperature comparison at Sacramento Station (purple is observation and blue is model).

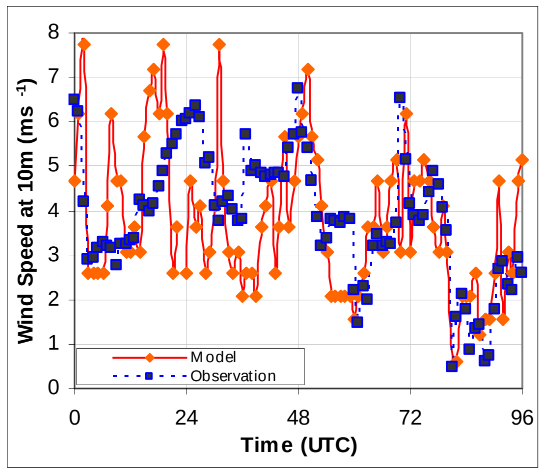

Fig. 5 Model versus observation surface wind speed comparison at Sacramento Station (orange is observation and blue is model).

5.2 Model Results

The first step in the analysis of the RAMS model results was taken by examining wind fields every hour for the two simulation cases. The three dimensional evolution of the sea breeze over the San Francisco Bay region was analyzed at the surface level. Horizontal slices of wind and temperature fields were plotted at 1000mb. Higher resolution wind fields (grid 3) were analyzed during this simulation period to examine the complex three-dimensional structures of the sea breeze and mountain-valley winds in this area. Analysis of the horizontal wind was carried out at the 1000 mb level. The analysis was done to better understand the dynamics of the region extending to the Sierra Nevada Mountains. For grid four, the analysis examined the dynamics of the local effects, and was focused over the city of Sacramento. Surface evolution of the sea breeze for this case showed similar flow to the observed wind profiler sea breeze.

During 1800 UTC 18 June 2005, the sea breeze has started to develop around the Central California coastal region. Westerly flow started to develop over the San Francisco bay and channeled towards the Carquinez strait. Upslope winds were developing over the coastal mountains with convergence over the mountaintops.

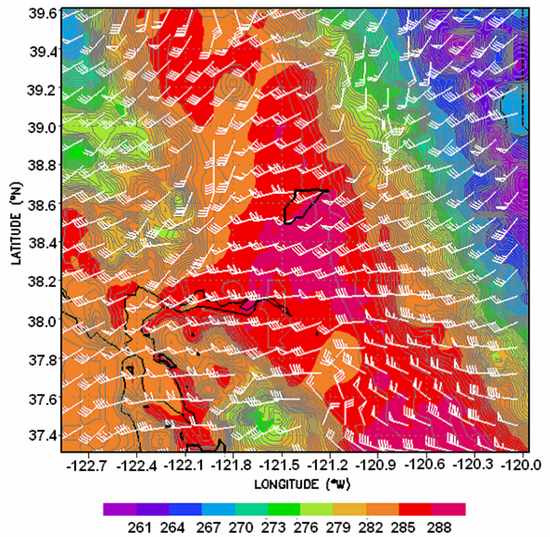

Fig. 6 0000 UTC 19 June 2005, temperature and wind fields of grid 3 (flag=5 m s^{-1}; barb= 1 m s^{-1} and half barb= 0.5 m s^{-1}).

As the day progressed, the sea breeze and the upslope winds peaked at 0000 UTC 19 June (Fig. 6), the sea breeze had strengthened to 4-8 m s^{-1} and had filled the Carquinez strait heading to the San Joaquin Valley. The sea breeze in the San Francisco Bay was stronger and penetrated far inland, being channeled through the Carquinez strait where the flow then joined the upslope winds on the eastern slopes of the Sierra Nevada. By 1200 UTC 19 June 2005 (Fig. 7), the sea breeze had diminished, and had started its retreat back to coastal waters. Down slope winds from the eastern part of the Sierras and western part of the coastal mountains created convergence zones over the Northern Central valley including Sacramento. Wind speeds were light and variable all over the region, ranging from 3 – 4 m s^{-1}. It can be notes from these two figures that temperatures were lower at the coastal and Sierra Mountains and higher over the Central Valley. During 0000 UTC 18 June 2005 the highest temperatures were south of Sacramento city and during the night the ocean is warmer.

In order to analyze the effect of land use change between case 1 and case 2 of this research study, difference maps of the wind and temperatures were produced. During 0000 UTC 19 June 2005 (Fig. 8), the high resolution (grid 4) plot of wind and temperature difference maps of case 1 and case 2 show an increase on both the wind and temperature fields. Heat had been advected from the city towards the eastern side of the Sierras with the increase heat island increasing the sea breeze from the Central Valley. The increase in the winds is 1- 2 m/s and the increase in temperatures is 0.5 to 1 ^{0}C. It is interesting to see that during 1200 UTC 19 June 2005, the heating had been localized to the central part of the city with the down slope winds from the eastern side of the Sierras and the western part of the coastal mountains converge at the central part of the city (Fig. 9).

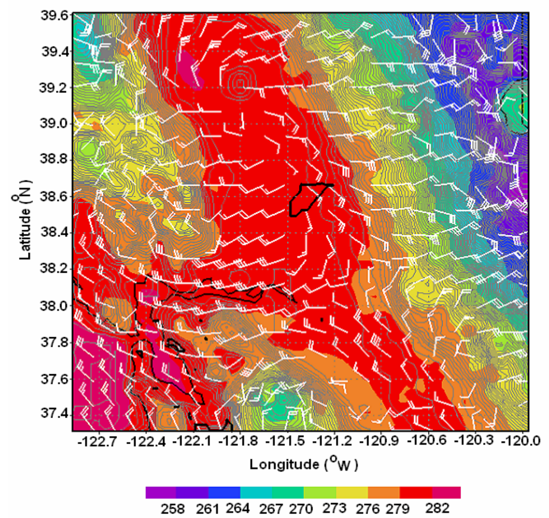

Fig. 7 1200 UTC 19 June 2005, temperature and wind fields of grid 3 (flag=5 m s^{-1}; barb= 1 m s^{-1} and half barb= 0.5 m s^{-1}).

5. SUMMARY AND CONCLUSIONS

Results of an atmospheric regional simulation focused in Northern California coast were presented for two land cover and land use scenarios namely the present LCLU scenario and the potential natural LCLU scenario. Results clearly indicate temperature and se breeze increases at the time when the sea breeze and UHI are expected to peak (15-18 local time). Results also clearly indicated temperature increases in the order of 0.8-1.0°C on the hills east of Sacramento. This temperature increase generates a low pressure that accelerates the sea breeze from the San Francisco Bay Area. The warm sea breeze increased is mixed with additional cold air from the Sierra Nevada generating a mixing and convergence zone caused by the changes in land cover. The net wind speed increase ranges between 1 and 6 m/s.

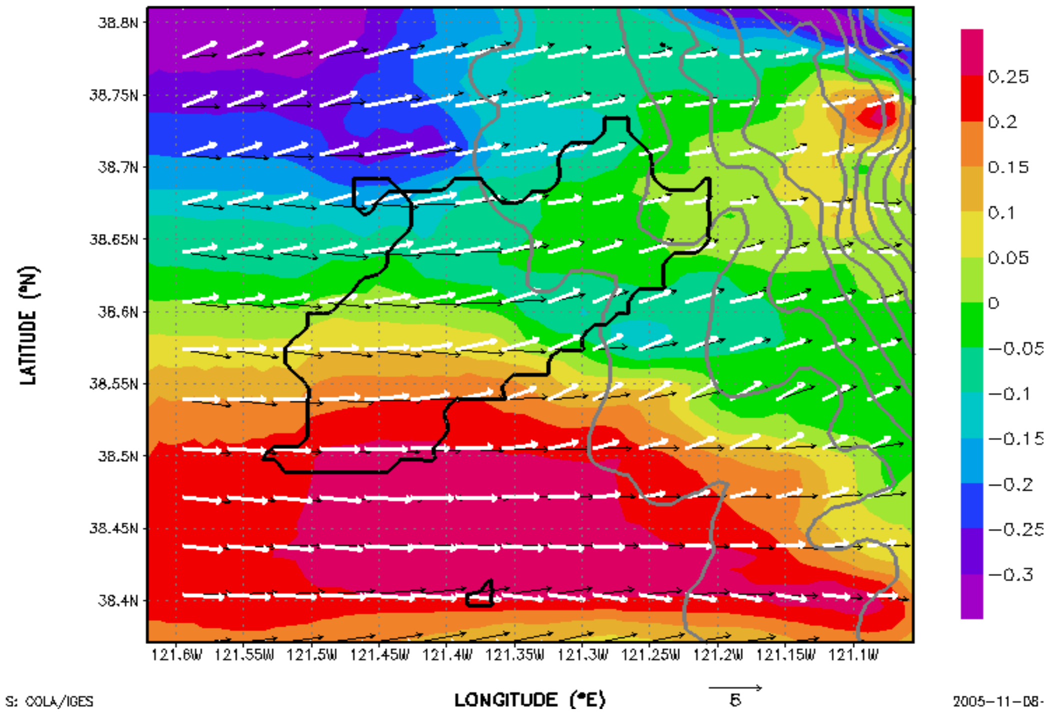

Fig. 8 0000 UTC 19 June 2005, Simulated wind and difference maps between case 1 and case 2. (black arrow is pre-urbanization, white arrow current version of the city)

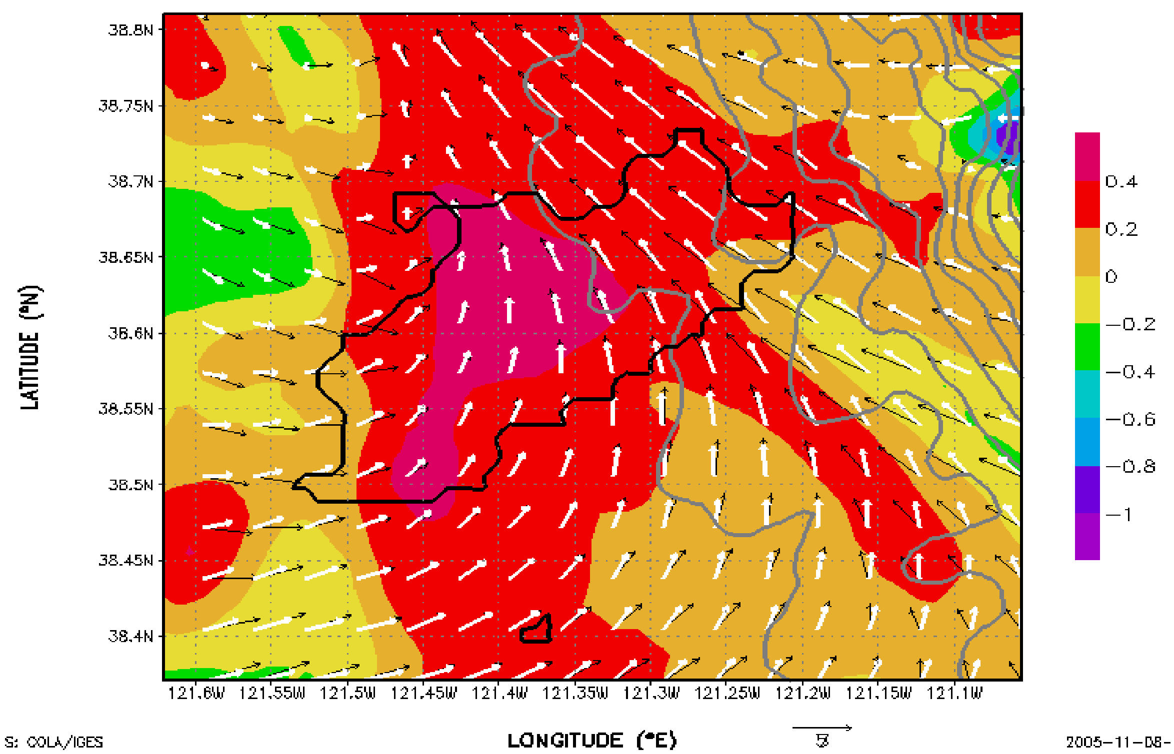

Fig. 9 1200 UTC 19 June 2005, Simulated wind and temperature difference maps between case 1 and case 2. (black arrow is pre-urbanization, white arrow current version of the city)

6. ACKNOWLEDGEMENTS

The authors would like to thank the School of Engineering of Santa Clara University for providing support a graduate student (Bereket Lebassi), to the Meteorology Program of San José State University for providing access to their supercomputers, and to the NASA Summer Faculty Fellowship program for providing financial support (J.E. González).

7. REFERENCES

Bornstein R.D., 1995. Observations of the urban heat island effect in New York City, *Journal of Applied Meteorology*, **14,** 1459-1477.

Bornstein, R. D., 1968: Observations of the urban heat island effect in New York City. *J Appl. Meteor.*, **7**, 575-582.

Lebassi Bereket, Clara University, Santa Clara, CA; and D. Fabris, J. E. Gonzalez, S. Zarantonello, S. Chiappari, N. L. Miller, and R. Bornstein, 2005: Climatology temperature mapping for California urban heat island study site selection, Atmospheric science and air.

Bridger, A. F. C., W. C. Brick, and P. F. Lester, 1993: The structure of the marine inversion layer of the central California coast: Mesoscale conditions*.* *Mon. Wea. Rev.*, **121**, 335-351.

Burk, S. and W. Thompson, 1996: The summertime low-level jet and marine boundary layer structure along the California coast. *J. Atmos. Sci.*, **50**, 3959-3982.

Dixon, P. G., and Mote, L. T., 2003. Patterns and causes of Atlanta's urban heat island-initiated precipitation, *J. Appl. Meteor*., **42**, pp. 1273-1284.

Jauregui, E., 1997. Heat island development in Mexico City. *J. Atmos. Env*., **31B**, pp. 3821-3831.

Gallo, K. P., A. L. McNab, T. R. Karl, J. F. Brown, J. J. Hood, and J. D. Tarpley, The use of a vegetation index for assessment of the urban heat island effect, *International Journal of Remote Sensing*, ***14***, 11, 2223-2230, 1993.

Klemp, J.B. and D.K. Lilly, 1978: Numerical simulation of hydrostatic mountain waves*. J. Atmos. Sci.,***35**, 78-107.

Lyons, W. A., Pielke, R. A., Tremback, C. J, Walko, R. L., Moon, D.A., Keen, C.S., 1995, Modeling impacts of messocale vertical motions upon coastal zone air pollution dispersion, *Atmospheric Environment*, **29**, pp. 283-301.

Mesinger, F. and A. Arakawa, 1976: Numerical methods used in atmos-pheric models. GARP Publication Series, No. 14, WMO/ICSU Joint Organizing committee, 64 pp.

Myrup, L. D., 1969: A numerical model of the urban heat island. *J. Appl Meteor.*, 16, 11-19.

Price, J. C., 1979: Assessement of the urban heat island effect through the use of satellite data. *Mon. Wea. Rev*., **107**, 1554-1557

Simpson, J. E., 1994: *Sea Breeze and Local Winds*. Cambridge University Press, 243 pp.

Tripoli, G. J., Cotton W. R., 1982: The Colorado State University three-dimentional cloud/mesoscale model – 1982. Part I: General theore-tical framework and sensitivity experiments. J*. de Rech. Atmos., ***16**, 185-220.

Tso, C. P., 1995. A survey of urban heat island studies in two tropical cities. *J. Atmos. Env*., **30**, pp. 507-519.

Walko, R. L., and Tremback, C. J., 2001: RAMS technical description. http://www.atmet.com/html/docs/rams/rams_techman.pdf

Pielke, R. A., 1984: *Mesoscale Meteorological Modeling.* Academic Press, CA 612 pp.

Pielke, R. A., 1974: A three-dimensional numerical model of the sea bree-ze over south Florida. *Mon. Wea. Rev.,* **102**, 115–139.